Research Square

Preprints are preliminary reports that have not undergone peer review.
They should not be considered conclusive, used to inform clinical practice,
or referenced by the media as validated information.

Expression Profiles of Plasma IFN Signaling-Related miRNAs (ISR-miRNAs) at the Acute and Recovery Phase of COVID-19

Jing Wu
Soochow University Medical College
Xingxiang Liu
Huai'an Fourth People's Hospital
Jianguo Shao
Nantong Third People's Hospital
Yuanyuan Zhang
Huai'an Fourth People's Hospital
Renfei Lu
Nantong Third People's Hospital
Hong Xue
Nantong Third People's Hospital
Yunfang Xu
Huai'an Fourth People's Hospital
Lijuan Wang
Huai'an Fourth People's Hospital
Hui Zhou
Suzhou Industrial Park Centers for Disease Control and Prevention
Lugang Yu
Suzhou Industrial Park Centers for Disease Control and Prevention
Ming Yue
Nanjing Medical University affiliated Nanjing Hospital: Nanjing First Hospital
Chen Dong (cdong@suda.edu.cn)
Soochow University Medical College https://orcid.org/0000-0001-5175-1662

Research Article

Keywords: COVID-19, MicroRNA, RBD-IgG, IFN-1 signaling pathway

Posted Date: June 7th, 2021

DOI: https://doi.org/10.21203/rs.3.rs-528348/v1

License: This work is licensed under a Creative Commons Attribution 4.0 International License.
Read Full License

Abstract

Background

Coronavirus disease 2019 (COVID-19) has brought major harm and challenges to the world. Although many studies have suggested that IFN-I could affect the life cycle of the virus by regulating the expression level of microRNAs, the expression characteristics of plasma IFN-I signaling-related miRNAs at the acute and recovery phase of COVID-19 remain unclear.

Methods

Demographic characteristics and fasting blood samples were collected from the acute and recovery phases of 29 COVID-19 patients and 29 healthy controls matched by age (± 5years) and gender (1:1). Expression levels of 12 IFN signaling-related miRNAs were analyzed using RT-qPCR. The receptor-binding domain (RBD) IgG antibody in the convalescent plasma samples was detected using competitive ELISA.

Results

Compared with healthy controls, patients with COVID-19 presented increased levels of miR-29b-3p (~ 5.91-fold), miR-497-5p (~ 2.28-fold), and miR-1246 (~ 7.97-fold), and decreased expression levels of miR-186-5p (~ 6.39-fold) and miR-15a-5p (~ 3.26-fold) at the acute phase of infection. However, the expression levels of miR-29b-3p and miR-1246, which significantly elevated at the acute phase, were not different between individuals at the recovery phase and healthy controls. The expression levels of miR-30b-5p, miR-497-5p, miR-409-3p and miR-548c-5p in convalescent plasma samples were significantly lower than those in healthy controls. However, the concentration of miR-186-5p in the convalescent plasma samples was significantly higher than that in healthy controls and patients with acute infection. Furthermore, competitive ELISA results showed that the plasma level of miR-497-5p at the acute phase positively correlated with RBD-IgG antibody response (r=0.48, *P*=0.038).

Conclusions

The present study firstly reported that timely and appropriate regulation of IFN signaling-related miRNA expression plays a critical role during both acute and recovery phase of SARS-CoV-2 infection. Furthermore, the circulating miR-497-5p level was positively correlated to RBD-IgG antibody response in COVID-19 patients.

Background

Coronavirus disease 2019 (COVID-19), caused by severe acute respiratory syndromecoronavirus-2 (SARS-CoV-2), has brought major harm and challenges to more than 200 countries and regions around the world [1]. According to the COVID-19 Data Repository by The Center for Systems Science and Engineering at Johns Hopkins University, as of 1 May 2021, there have been 151,409,122 laboratory-confirmed cases of COVID-19 with 3,180,624 deaths [2]. The number of people infected and died makes the COVID-19

pandemic one of the worst pandemics in recent years, and certainly worse than previous coronavirus pandemics such as SARS and MERS.

Type I interferon (IFN-I) exists in vertebrates and triggers the Januskinase/signal transducer and activator of transcription (JAK/STAT) signaling pathway with subsequent induction of IFN-stimulated genes (ISGs) [3]. Mounting studies have suggested that IFN-I could affect the life cycle of the virus by regulating the expression level of microRNAs (miRNAs), which are key post-transcriptional regulators in various cellular biological processes. For example, Aboulnasr*et al.* reported that IFN-α/β could induce the expression of miR-122 in hepatocytes. However, the reduction of miR-122 expression level could weaken the effect of IFN-a/β in inhibiting hepatitis C virus (HCV) [4]. However, many viruses could develop strategies to alter miRNA expression, thereby inhibiting the activity of IFN-I signaling pathway. The result from the sequence alignment illustrates that the presence of putative miRNA target sites for the IFN-I-induced miRNAs located in strictly conserved areas of the HCV genome. Pedersen *et al.* further confirmed that miR-196, miR-296, miR-351, miR-431 and miR-448 could bind to complementary sequences in the HCV genome and inhibit virus replication [5].

During the past year, several thousand studies have investigated the epidemiologic, clinical, biological and radiological characteristics of COVID-19 patients [6-8]. However, the mechanism of the new coronavirus infection has not yet been fully understood. Based on the prediction from miRDB (http://www.mirdb.org/) and miRPathDB (https://mpd.bioinf.uni-sb.de/overview.html), our recent analysis indicated that the genome of SARS-CoV-2 contains 12 candidate binding sites for IFN-I signaling-related miRNAs (ISR-miRNAs) (Table S1) [9,10]. Thus, to determine the role of ISR-miRNAs in the host response to SARS-CoV-2 infection, this study was conducted to analyze the expression characteristics of circulating ISR-miRNAs at the acute and convalescence phase of COVID-19 patients.

Materials And Methods

Study population This study was approved by the ethics committee of Huai'an Fourth Hospital (Huai'an, China), and conducted in accordance with the Declaration of Helsinki. Between January 2020 and May 2020, 29 COVID-19 patients at the acute phase of infection and 29gender and age (± 5years) matched healthy controls were recruited from Huai'an Fourth hospital. All participants signed an informed consent form and the participants coinfected with other viruses were excluded. The diagnosis of COVID-19 was based on the "New Coronavirus Pneumonia Prevention and Control Program (5th version)" published by the National Health Commission of China [11]. The demographic characteristics of acute COVID-19 patients and controls, including weight, height, and blood pressure were collected by face-to-face interview. In addition, the data about clinical signs, symptoms, and potential comorbidities were extracted retrospectively from electronic medical records. Blood sample collection and laboratory analysis Five milliliters of acute phase blood sample was collected from each patient after at least 8 hours fasting during patients' first admission to the hospital. Three months after discharge, the patients were invited to participate in the following-up survey and the convalescence fasting blood samples were collected. In addition, five milliliters of fasting blood samples were collected from the recruited age- and gender-

matched healthy controls. All blood samples were centrifuged at 3000 g for 10 minutes at room temperature. Plasmas were separated and inactivated in a water bath at 56°C for 30 minutes, and then frozen at -80 °C for storage as quickly as possible. The routine laboratory tests, including lymphocyte (LYM) count, neutrophil (NEUT) count, white blood cell (WBC) count, platelet (PLT) count, ALT and AST were determined using commercial reagents according to the manufacturer's instructions. ISR-miRNA selection In this study, the complete genome of SARS-CoV-2 strain (NC_045512.2) was retrieved from the GenBank database and used as a reference sequence. The miRDB (http://www.mirdb.org/) software was firstly used to identify miRNAs which can target the genome of SARS-CoV-2 (NC_045512.2). The miRNAs with more than 95 of the target score were primarily included [12,13]. Then, we used miRPathDB (https://mpd.bioinf.uni-sb.de/overview.html) to identify miRNAs related to the JAK-STAT pathway [14]. Furthermore, we conducted a systematic literature review to identify the ISR-miRNAs using the following terms “JAK”, “STAT”, and “JAK/STAT” in PubMed. Finally, twelve miRNAs were selected as ISR-miRNAs for the present analysis: let-7c-5p, miR-15a-5p, miR-15b-5p, miR-29b-3p, miR-30b-5p, miR-146b-3p, miR-148a-3p, miR-186-5p, miR-409-3p, miR-497-5p, miR-548c-5p and miR-1246. The detailed information about the selected 12 ISR-miRNAs were shown in Table S1. Plasma RNA extraction and ISR-miRNA quantitation analysis Total RNA was isolated from 300 μL plasma with a commercial RNA extraction and purification kit (MACHEREYNAGEL SA, France) according to the manufacturer’s protocol. To warrant consistency in the experimental procedures, exogenous cel-miR-39 was spiked into each serum sample before RNA extraction and used as an internal control for normalizing miRNA expression levels. The concentration of RNA was measured at OD260/280 by a NanoDrop ND-1000 spectrophotometer (Thermo Scientific, Wilmington, Delaware). All real-time PCR was performed on a Q6 Real-Time System (Applied Biosystems) using the SYBR Green-based real-time detection method. The miDETECTA TrackTM miRNA qRT-PCR Starter Kit, the upstream and downstream primers for selected ISR-miRNAs quantitation were ordered from RiboBio Corporation (Guangzhou, China) [15]. As described above, cel-miR-39 miDETECTTM miRNA External Control (RiboBio, China) was selected as an endogenous control for miRNA expression analysis. In this study, the reaction system for ISR-miRNA Poly(A) tailing contained 1 μg of total small RNA, 2 μL 5X Poly(A) polymerase buffer, 1 μL Poly(A) polymerase and RNase-free water up to 10 μL. The reaction system for reverse transcription contained 4 μL RTase mix, 4 μL 5X RTase buffer, 2 μL miDETECT A TrackTM Uni-RT Primer and 10 μL Poly(A) Tailing product. 20 μL reaction system for real-time quantitative PCR contained 0.5 μL miDETECT A TrackTM miRNA Forward Primer (10μM), 0.5 μL miDETECT A TrackTM Uni-Reverse Primer (10μM), 10 μL 2X SYBR Green Mix, 0.04 μL ROX Reference Dye, 2 μL cDNA and RNase-free water. The cycle threshold (CT value) was defined as the number of cycles required for the fluorescent signal to cross the threshold. The expression of ISR-miRNA relative to cel-miR-39 miRNA was reported as dCT (ΔCT), which was calculated by subtracting the Ct of cel-miR-39 from the Ct of target ISR-miRNA. The relative quantitative of each ISR-miRNA was expressed as 2(-ΔCT), and was transformed into their natural logarithm to eliminate heteroscedasticity. The significance of ISR-miRNA expression between different groups was defined as a difference of at least 2-fold when compared with healthy controls. Competitive ELISA for receptor-binding domain (RBD) IgG antibody detection The competitive ELISA steps were carried out using “RBD-IgG antibody detection kit” (Beijing, China) according to the manufacturer’s introduction. Briefly, 96-well Corning Costar high binding

plates were coated with SARS-CoV-2 spike RBD protein at a concentration of 0.1 μg per well. For the RBD-IgG antibody measurement, 50 μL of 1:50 diluted plasma sample and 50 μL of HRP-conjugated ACE2-mFc (0.2 μg/ml) were added into each well. Meanwhile, two negative and two positive plasma controls and two blank wells incubated with HRP-conjugated ACE2-mFc were included on each plate, respectively. After incubated for 30 minutes, the plate was washed three times and TMB substrate solution was added. The reaction was stopped after 15 minutes by the addition of 2M H2SO4. The OD at 450 nanometers was measured with an EMax Plus microplate reader (Molecular Devices, San Jose, CA). Results were expressed as percent inhibition (PI), calculated using the following formula: PI =100% × [1 – (sample OD-blank OD)/(negative control OD-blank OD)]. The sample with more than 25% of PI was considered as anti-RBD IgG positive. Statistical analysis Data were presented as means ± SD for skewed quantitative data and proportions for categorical data as indicated. Comparisons of differences in categorical data between groups were performed using $\chi 2$ test or Fisher's exact test, as appropriate. Kruskal-Wallis H test and Dunn-Bonferroni test were used to analyze the clinical parameters among healthy controls, patients at the acute and recovery phases of COVID-19. Pearson correlation was done to measure the correlations between ISR-miRNAs and clinically relevant parameters at the acute phase of COVID-19, as well as the RBD-IgG antibody levels at the recovery phase of disease. All statistical tests were two-tailed and a probability level of $P< 0.05$ was considered as statistically significant. Data were analyzed using SAS 9.4 software (SAS Institute, Cary, NC, USA).

Results

Demographic and clinical characteristics of included participants

The demographic and clinical characteristics of the included COVID-19 patients were summarized in Table 1. The mean (±standard deviation) age of the patients with COVID-19 was 47.45±15.72 years, and 58.62% were male. Moreover, three, nine and one patient had pre-existing diabetes, hypertension and renal insufficiency, respectively. At the acute phase, the most common symptom at the onset of illness was fever (75.86%). In addition, the median incubation period was 5.0 days. The virus nucleic acid test turned negative approximately 7 days after admission.

Compared with the healthy controls, patients with COVID-19 presented lower LYM counts (Z=-3.86, *P*=0.001) and PLT counts (Z=-2.80, *P*=0.005) at the acute phase of disease. In addition, LYM, PLT and CD8+ T cell counts at the recovery phase were significantly higher than those at the acute phase. However, we did not observe the difference in other clinical parameters among the three groups.

Expression profiles of ISR-miRNAs at the acute phase of COVID-19

Changes in the relative expression of twelve miRNAs were measured and presented in Figure 1. Compared with healthy controls, patients with COVID-19 were more likely to have elevated levels of miR-29b-3p (~ 5.91-fold), miR-497-5p (~ 2.28-fold) and miR-1246 (~ 7.97-fold), and decreased expression levels of miR-186-5p (~ 6.39-fold) and miR-15a-5p (~ 3.26-fold) at the acute phase of infection. Then, we looked for correlations with parameters clinically relevant to the included ISR-miRNAs. Results showed

that miR-30b-5p negatively correlated with CD4+ T cell counts (r=-0.41, *P*=0.030) in patients with acute SRAS-CoV-2 infection.

Expression profiles of ISR-miRNAs at the recovery phase of COVID-19

As the results shown in Figure 1, the expression levels of miR-29b-3p and miR-1246, which significantly elevated at the acute phase, were not different between individuals at the recovery phase and healthy controls. However, the results showed that the expression levels of miR-30b-5p, miR-409-3p, miR-497-5p and miR-548c-5p in convalescent plasma samples were significantly lower than those in healthy controls. In addition, the concentration of miR-186-5p in convalescent plasma samples was significantly higher than that in healthy controls and patients with acute infection. No significant difference was found in the relative expression levels of other ISR-miRNAs among the recovery individuals, patients who acute SRAS-CoV-2 infection and healthy controls.

Association of ISR-miRNAs with RBD-IgG antibody at the recovery phase

Among 28 patients who provided enough convalescent plasma samples, RBD-IgG antibodies were detected in 27 COVID-19 patients using competitive ELISA. The highest and lowest PI values were 93.0% and 41.2% (median PI: 77.5%), respectively. The potential association of circulating ISR-miRNA levels with RBD-IgG antibody response was further analyzed in the present study. As the results showed in Fig 3, the plasma level of miR-497-5p at the acute phase positively correlated to RBD-IgG antibody response (*r*=0.48, *P*=0.038). However, no correlation was observed between other ISR-miRNAs and RBD-IgG response in the analyzed patients.

Table1. Demographics, baseline characteristics of COVID-19 patients and healthy controls

Characteristics	Healthy controls	Acute phase	Convalescent phase	*P*	P_a	P_b
Age, years	48.34±13.50	47.45±15.72	47.45±15.72	0.817		
Male, n(%)	14 (48.28)	17 (58.62)	17 (58.62)	0.430		
BMI, kg/cm^2	24.41±4.32	26.40±3.84	25.66±3.26	0.151		
Signs and symptoms						
Fever	None	22 (75.86)	None			
Cough	None	14 (48.27)	None			
Myalgia or fatigue	None	2 (6.90)	None			
Expectoration	None	2 (6.90)	None			
Headache	None	1 (3.44)	None			
Oppression in chest	None	2 (6.90)	None			
Incubation period (days)	None	5.0 (4.0, 7.0)	None			
Days from first admission to transfer	None	7.0 (4.0, 8.5)	None			
Underlying						
Hypertension	0 (0.00)	9 (31.03)	9 (31.03)			
Diabetes	0 (0.00)	3 (10.34)	3 (10.34)			
Laboratory findings						
WBC, ×10^9/L	5.77 (5.13, 6.17)	5.27 (4.21, 6.80)	4.87 (4.09, 6.50)	0.407	0.335	0.632
NEUT, ×10^9/L	3.28 (2.46, 4.02)	3.32 (2.49, 4.93)	2.95 (2.45, 4.03)	0.649	0.619	0.372
LYM, ×10^9/L	1.98 (1.61, 2.12)	1.07(0.81, 1.49)	1.59 (1.26, 1.99)	<0.001	0.001	0.007
HB, g/L	132 (122, 149)	144 (133, 151)	141 (134,148)	0.117	0.074	0.897
PLT, ×10^9/L	214 (182, 253)	176 (149, 198)	183 (143, 219)	0.010	0.005	0.740
Cr, μmol/L	56.4 (51.7, 70.4)	65.3 (51.9, 85.5)	68.0 (56.6, 80.8)	0.139	0.113	0.971
ALT >40 U/L, n	2 (13.33)	6 (40.00)	7 (46.67)	0.184		
AST >40 U/L, n	0 (0.00)	7 (87.50)	1 (12.50)	0.654		

CD4, /μL	433 (272, 743)	550 (451, 800)	0.086
CD8, /μL	292 (171, 455)	467 (323, 631)	0.003

P_a: Healthy controls *vs* Acute phase; P_b: Acute phase *vs* Convalescent phase.

Discussion

Previously, many studies have reported that ISR-miRNAs were significantly associated with viral infection [3-5]. For example, Bandyopadhyay *et al.* found that miR-29 overexpression in LX-2 cells could decrease collagen expression. However, miR-29 downregulation by HCV might depress extracellular matrix synthesis during activation of hepatic stellate cells [16]. In a study in Demark, Lajer *et al.* reported that increased levels of miR-497 significantly increased in HPV+ HNSCC patients compared with patients having HNSCC without HPV infection [17]. In addition, Xu *et al.* reported that the expression level of miR-1246 could be specifically induced by HEV71 in human neuroblastoma cells [18]. Similar to these findings, our results suggested that the expressions of miR-29b-3p, miR-497-5p and miR-1246 were significantly upregulated, indicating that these ISR-RNAs might play an important role in the pathogenesis of acute SARS-CoV-2 infection.

This study revealed that the expression levels of miR-186-5p and miR-15a-5p significantly decreased at the acute phase of COVID-19 patients. Following in silico target prediction and pathway enrichment analyses, Zhao *et al.* suggested that miR-186-5p was depleted in retroviral infection. However, the increased miR-186-5p expression could inhibit HIV infection by immunoregulation and T cell regulation [19]. Moreover, Wu *et al.* reported that overexpressed miR-186 could inhibit the JAK/STAT signaling pathway *in vitro* [20]. The results from the most recent study reported that hsa-miR-15b-5p were significantly downregulated in hamster lung samples infected by SARS-CoV-2 [21]. Considering that the miR-15 family members (i.e., miR-15a, 15b) possess the same seed sequence and have the same target genes, the present results further suggested that downregulated expression of miR-186-5p and miR-15a-5p might be helpful for the IFN-I signaling pathway activation at the acute phase of SARS-CoV-2 infection.

In the early phase of viral infection, the host's innate immunity, including IFN-I signaling pathway, is the first defense mechanism [22]. However, since the excessive cytokines produced by IFN-1 signaling can cause a cytokine storm and damage the body [23], the effective and precise regulation of JAK/STAT signaling activity is very important for the patients recovered from acute infection [20,24-27]. Therefore, it is not a surprise that the expression levels of miR-30b-5p, miR-409-3p, miR-497-5p and miR-548c-5p significantly decreased, while miR-186-5p expression significantly increased in convalescent plasma samples when compared with those of healthy controls and acute infected patients. Although the exact timing during IFN-I-activated feedback regulation and control of JAK/STAT signaling is currently unclear,

the present results implicated that a timely and appropriate JAK-STAT signaling regulation should be necessary and helpful for the recovery of patients with SARS-CoV-2 infection.

A large number of studies have confirmed that the interaction between RBD located at the spike protein of SARS-CoV-2 and the receptor ACE2 on host cells is essential for viral entry [28,29]. Therefore, antibodies against RBD at the recovery phase of COVID-19 present neutralizing activity because they can block the interaction between ACE2 and viral spike protein [30]. Previously, Premkumar *et al.* reported that antibodies targeting RBD accounted for more than 90% of neutralizing activity in the convalescent serum [31]. In the present study, competitive ELISA results showed that 27/28 patients developed RBD-IgG antibodies at the recovery phase. Moreover, results of the present study suggested that the plasma level of miR-497-5p at the acute phase positively correlated to RBD-IgG antibody response at the recovery phase, indicating that miR-497-5p might serve as a candidate ISR-miRNA for the prediction of SARS-CoV-2 neutralization antibody.

This study has several limitations. First, considering that only 29 patients were included in this analysis, caution should be taken when interpreting the present findings. Moreover, the difference in plasma ISR-miRNAs between patients with mild and severe infection could not be explored because of the small sample size. Second, although we, for the first time, reported that miR-29b-3p, miR-497-5p, miR-1246, miR-186-5p and miR-15a-5p were significantly associated with acute SARS-CoV-2 infection, more miRNAs related to JAK/STAT pathway still need to be thoroughly analyzed in the future. Moreover, to understand the questions behind the observed associations, the role of ISR-miRNAs involved in the pathogenesis of COVID-19 should be investigated in both *in vivo* and *in vitro* studies. Finally, since the disease progression and antibody response might be influenced by various risk factors (age, comorbidity disease such as hypertension and diabetes) [32-34], the effects of the ISR-miRNAs and interactions of other risk factors on SARS-CoV-2 infection should also be carefully verified in the future.

Conclusions

In summary, this study is the first to report that appropriate regulation of ISR-miRNA expression plays a critical role during both acute and recovery phases of SARS-CoV-2 infection. Furthermore, the circulating miR-497-5p level was positively correlated to RBD-IgG antibody response in COVID-19 patients. In the future, further studies with large study samples are needed to understand the biological significance of ISR-miRNAs during SARS-CoV-2 infection.

Abbreviations

COVID-19: Coronavirus disease 2019; SARS-CoV-2: Severe acute respiratory syndrome coronavirus-2; IFN-1: Type I interferon; JAK-STAT: Januskinase/signal transducer and activator of transcription; ISGs: IFN-stimulated genes; HCV: Hepatitis C virus; ISR-miRNAs: IFN-I signaling-related miRNAs; LYM: Lymphocyte; NEUT: Neutrophil; WBC: White blood cell; PLT: Platelets; ALT: Alanine aminotransferase; AST: Aspartate aminotransferase; RBD: Receptor-binding domain; PI: Percent inhibition

Declarations

Ethics approval and consent to participate

This study was approved by the ethics committee of Huai'an Fourth Hospital, Huai'an, China (Ethics Certification Number: HASY2020004), and written informed consent was obtained from each participant.

Consent for publication

Not applicable

Availability of data and materials

The data and material included in the present study could be provided by Chen Dong (cdong@suda.edu.cn) and Jing Wu (20194247006@stu.suda.edu.cn).

Competing interests

The authors declare that they have no conflicts of interest.

Funding

This work was supported by the National Natural Science Foundation of China (No. 81773507). Special Foundation for COVID-19 from Soochow University (JJ13900420). The Foundation of Technology Program in Soochow (SYS2020049).

Authors' contributions

MY and CD conceived and designed the study. JW, XL, JS, YZ, RL, YX, LW and HX collected the samples. JW, XL, JS and HZ generated the sequencing data. JW, XL, LY, MY and CD analyzed the data, carried out the computational analysis, interpreted the data, and drafted the manuscript.

Acknowledgments

We gratefully acknowledge Yun Zhang, Yonghong Zhang and other volunteers who participated in our study.

References

1. O'Driscoll M, Ribeiro Dos Santos G, Wang L, Cummings DAT, Azman AS, Paireau J, et al. Age-specific mortality and immunity patterns of SARS-CoV-2. Nature. 2021;590(7844):140-45.
2. COVID-19 Data Repository by the Center for Systems Science and Engineering (CSSE) at Johns Hopkins University. Available at: https://www.arcgis.com/apps/opsdashboard/index.html#/bda7594740fd40299423467b48e9ecf6 . Accessed May 1, 2021.

3. Wang Y, Zhu P, Qiu J, Wang J, Zhu H, Zhu Y, et al. Identification and characterization of interferon signaling-related microRNAs in occult hepatitis B virus infection. Clin Epigenetics. 2017;9:101.
4. Aboulnasr F, Hazari S, Nayak S, Chandra PK, Panigrahi R, Ferraris P, et al. IFN-λ inhibits miR-122 transcription through a Stat3-HNF4α inflammatory feedback loop in an IFN-α resistant HCV cell culture system. PLoS One. 2015;10(12):e0141655.
5. Pedersen IM, Cheng G, Wieland S, Volinia S, Croce CM, Chisari FV, et al. Interferon modulation of cellular microRNAs as an antiviral mechanism. Nature. 2007;449(7164):919-22.
6. Hu B, Guo H, Zhou P, Shi ZL. Characteristics of SARS-CoV-2 and COVID-19. Nat Rev Microbiol. 2021;19(3):141-54.
7. Guan WJ, Ni ZY, Hu Y, Liang WH, Ou CQ, He JX, et al. Clinical characteristics of coronavirus disease 2019 in China. N Engl J Med. 2020;382(18):1708-20.
8. Jiang H, Guo W, Shi Z, Jiang H, Zhang M, Wei L, et al. Clinical imaging characteristics of inpatients with coronavirus disease-2019 in Heilongjiang Province, China: a retrospective study. Aging (Albany NY). 2020;12(14):13860-68.
9. Arisan ED, Dart A, Grant GH, Arisan S, Cuhadaroglu S, Lange S, et al. The prediction of miRNAs in SARS-CoV-2 genomes: hsa-miR databases identify 7 key miRs linked to host responses and virus pathogenicity-related KEGG pathways significant for comorbidities. Viruses. 2020;12(6):614.
10. Fulzele S, Sahay B, Yusufu I, Lee TJ, Sharma A, Kolhe R, et al. COVID-19 virulence in aged patients might be impacted by the host cellular microRNAs abundance/profile. Aging Dis. 2020;11(3):509-22.
11. National Health Commission of the People's Republic of China. Diagnosis and treatment of new coronavirus pneumonitis. (trial version 5). http://www.nhc.gov.cn/yzygj/s7653p/202002/3b09b894ac9b4204a79db5b8912d4440.shtml.
12. Chen Y, Wang X. miRDB: an online database for prediction of functional microRNA targets. Nucleic Acids Res. 2020;48(D1):D127-D131.
13. Wang JD, Zhou HS, Tu XX, He Y, Liu QF, Liu Q, et al. Prediction of competing endogenous RNA coexpression network as prognostic markers in AML. Aging (Albany NY). 2019;11(10):3333-47.
14. Kehl T, Kern F, Backes C, Fehlmann T, Stöckel D, Meese E, et al. miRPathDB 2.0: a novel release of the miRNA pathway dictionary database. Nucleic Acids Res. 2020;48(D1):D142-D147
15. Liu L, Liu Y, Feng C, Chang J, Fu R, Wu T, et al. Lithium-containing biomaterials stimulate bone marrow stromal cell-derived exosomal miR-130a secretion to promote angiogenesis. Biomaterials. 2019;192:523-36.
16. Bandyopadhyay S, Friedman RC, Marquez RT, Keck K, Kong B, Icardi MS, et al. Hepatitis C virus infection and hepatic stellate cell activation downregulate miR-29: miR-29 overexpression reduces hepatitis C viral abundance in culture. J Infect Dis. 2011;203(12):1753-62.
17. Lajer CB, Garnæs E, Friis-Hansen L, Norrild B, Therkildsen MH, Glud M, et al. The role of miRNAs in human papilloma virus (HPV)-associated cancers: bridging between HPV-related head and neck cancer and cervical cancer. Br J Cancer. 2012;106(9):1526-34.

18. Xu LJ, Jiang T, Zhao W, Han JF, Liu J, Deng YQ, et al. Parallel mRNA and microRNA profiling of HEV71-infected human neuroblastoma cells reveal the up-regulation of miR-1246 in association with DLG3 repression. PLoS One. 2014;9(4):e95272.
19. Zhao Z, Muth DC, Mulka K, Liao Z, Powell BH, Hancock GV, et al. miRNA profiling of primate cervicovaginal lavage and extracellular vesicles reveals miR-186-5p as a potential antiretroviral factor in macrophages. FEBS Open Bio. 2020;10(10):2021-39.
20. Wu DM, Wen X, Wang YJ, Han XR, Wang S, Shen M, et al. Effect of microRNA-186 on oxidative stress injury of neuron by targeting interleukin 2 through the janus kinase-signal transducer and activator of transcription pathway in a rat model of Alzheimer's disease. J Cell Physiol. 2018;233(12):9488-502.
21. Kim WR, Park EG, Kang KW, Lee SM, Kim B, Kim HS. Expression analyses of microRNAs in hamster lung tissues infected by SARS-CoV-2. Mol Cells. 2020;43(11):953-63.
22. Schreiber G. The role of Type I interferons in the pathogenesis and treatment of COVID-19. Front Immunol. 2020;11:595739.
23. Olbei M, Hautefort I, Modos D, Treveil A, Poletti M, Gul L, et al. SARS-CoV-2 causes a different cytokine response compared to other cytokine storm-causing respiratory viruses in severely Ill patients. Front Immunol. 2021;12:629193.
24. Lin X, Yu S, Ren P, Sun X, Jin M. Human microRNA-30 inhibits influenza virus infection by suppressing the expression of SOCS1, SOCS3, and NEDD4. Cell Microbiol. 2020;22(5):e13150.
25. Zhang CS, Lin Y, Sun FB, Gao J, Han B, Li SJ. miR-409 down-regulates Jak-Stat pathway to inhibit progression of liver cancer. Eur Rev Med Pharmacol Sci. 2019;23(1):146-54.
26. Wang J, Lin M, Ren H, Yu Z, Guo T, Gu B. Expression and clinical significance of serum miR-497 in patients with acute cerebral infarction. Clin Lab. 2019;65(4). doi: 10.7754/Clin.Lab.2018.181001.
27. Xing TJ, Xu HT, Yu WQ, Wang B, Zhang J. MiRNA-548ah, a potential molecule associated with transition from immune tolerance to immune activation of chronic hepatitis B. Int J Mol Sci. 2014;15(8):14411-26.
28. Kathiravan MK, Radhakrishnan S, Namasivayam V, Palaniappan S. An overview of spike surface glycoprotein in severe acute respiratory syndrome-coronavirus. Front Mol Biosci. 2021;8:637550.
29. Kadam SB, Sukhramani GS, Bishnoi P, Pable AA, Barvkar VT. SARS-CoV-2, the pandemic coronavirus: Molecular and structural insights. J Basic Microbiol. 2021;61(3):180-202.
30. Collins DP, Steer CJ. Binding of the SARS-CoV-2 spike protein to the asialoglycoprotein receptor on human primary hepatocytes and immortalized hepatocyte-like cells by confocal analysis. Hepat Med. 2021;13:37-44.
31. Premkumar L, Segovia-Chumbez B, Jadi R, Martinez DR, Raut R, Markmann A, et al. The receptor binding domain of the viral spike protein is an immunodominant and highly specific target of antibodies in SARS-CoV-2 patients. Sci Immunol. 2020;5(48):eabc8413.
32. Wu J, Zhang J, Sun X, Wang L, Xu Y, Zhang Y, et al. Influence of diabetes mellitus on the severity and fatality of SARS-CoV-2 (COVID-19) infection. Diabetes Obes Metab. 2020;22(10):1907-14.

33. Zhang J, Wu J, Sun X, Xue H, Shao J, Cai W, et al. Association of hypertension with the severity and fatality of SARS-CoV-2 infection: A meta-analysis. Epidemiol Infect. 2020;148:e106.
34. Savoia C, Volpe M, Kreutz R. Hypertension, a moving target in COVID-19: current views and perspectives. Circ Res. 2021;128(7):1062-79.

Figures

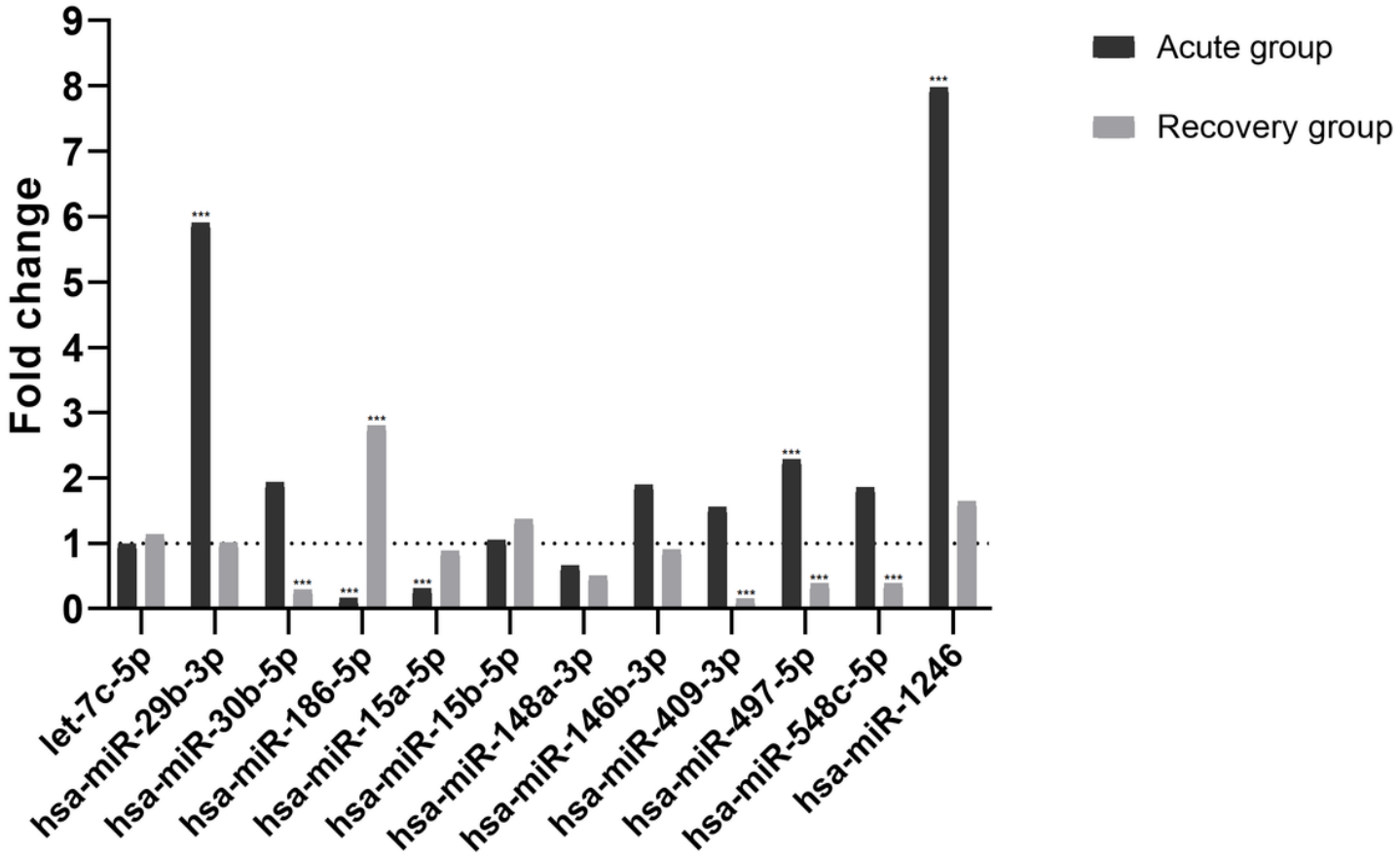

Figure 1

Fold changes of relative expression of twelve ISR-miRNAs in patients at the acute and recovery phase of COVID-19. The significance of ISR-miRNAs expression was defined as a difference of at least 2-fold when compared with healthy controls.

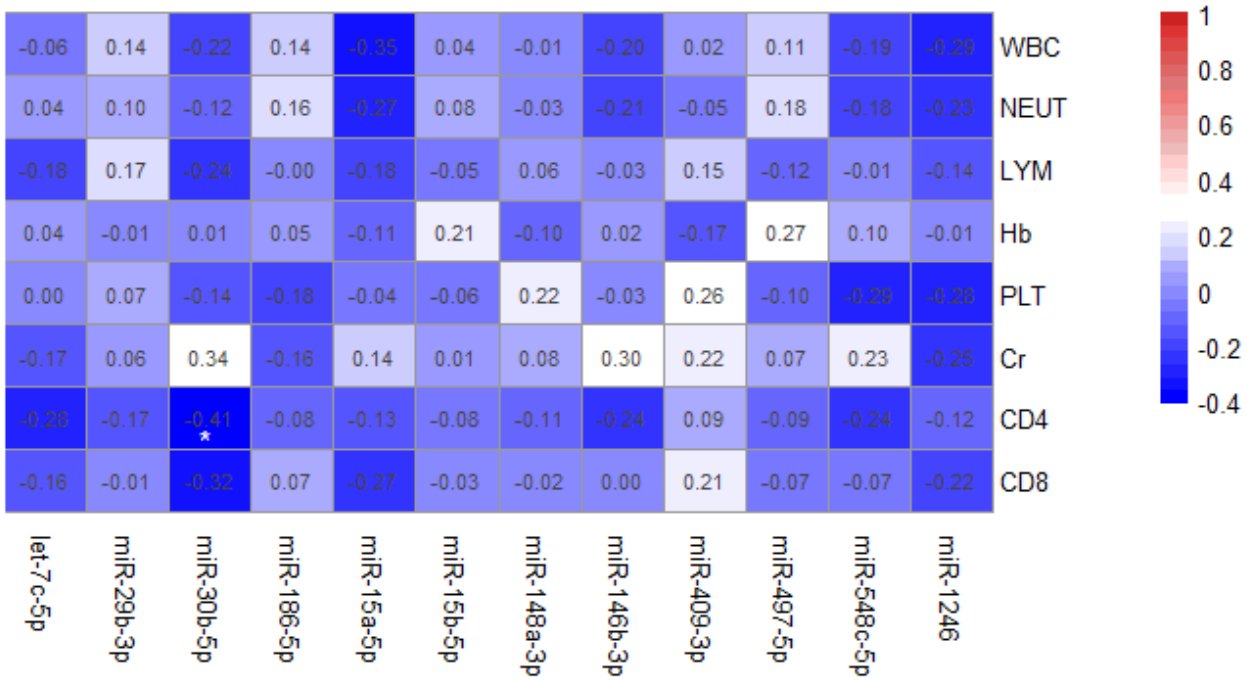

Figure 2

Pearson correlation between the relative expression levels of twelve ISR-miRNAs and WBC, NEUT, LYM, Hb, PLT, Cr, CD4+ and CD8+ T cells at acute phase of SAR-CoV-2 infection. The values in each square are correlation coefficient (r) of each group samples. The dendrogram on the right reveals the sample's correlation.

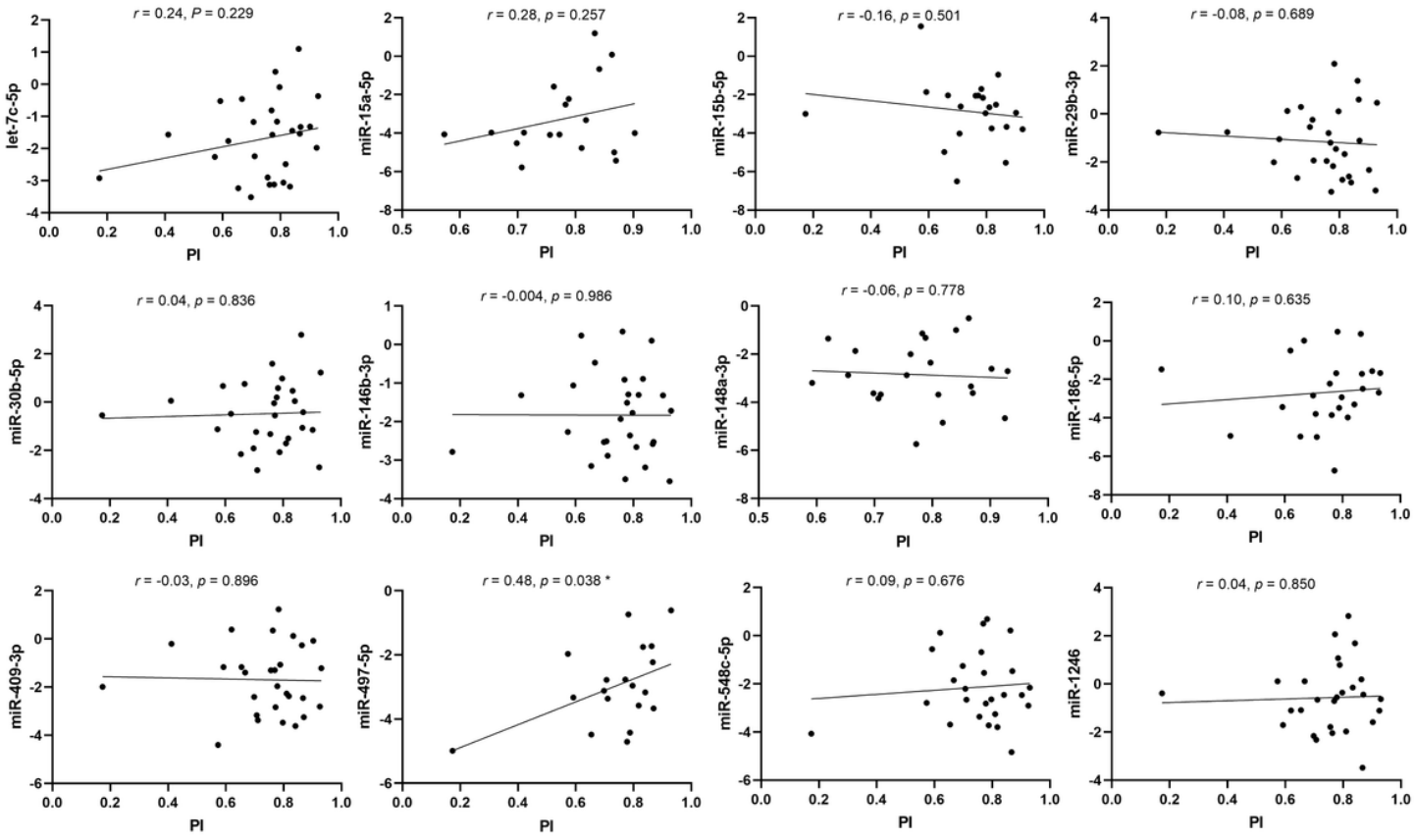

Figure 3

Pearson correlation between the relative expression levels of twelve ISR-miRNAs at acute phase of SARS-CoV-2 infection and RBD-IgG antibody response at the recovery phase of COVID-19.

Supplementary Files

This is a list of supplementary files associated with this preprint. Click to download.

- TableS1.ListofincludedmiRNAs.xlsx